Lab Invest 105 (2025) 104166

LABORATORY INVESTIGATION

journal homepage: https://laboratoryinvestigation.org/

Research Article

Role of Reserve Cells in Metaplasia and the Development of Human Papillomavirus–Associated High-Grade Squamous Intraepithelial Lesions at the Cervical Transformation Zone

Ademola Aiyenuro[a], Heather Griffin[a], Konstanze Schichl[a], Tanvier Omar[b], Jaume Ordi[c,d], Helen Kelly[e], Caroline Walker[a], Marta del Pino[c,f], Kanan Desai[g], Silvia de Sanjosé[d,g,*], Mark Schiffman[g,*], John Doorbar[a,*]

[a] *Department of Pathology, University of Cambridge, United Kingdom;* [b] *Department of Anatomical Pathology, Faculty of Health Sciences, University of the Witwatersrand, Charlotte Maxeke Academic Hospital, Johannesburg, South Africa;* [c] *Institute Clinic of Gynecology, Obstetrics, and Neonatology-University of Barcelona, Barcelona, Spain;* [d] *IS Global, Barcelona, Spain;* [e] *London School of Hygiene and Tropical Medicine, London, United Kingdom;* [f] *Institut d'Investigacions Biomèdiques August Pi i Sunyer (IDIBAPS), Barcelona, Spain;* [g] *Division of Cancer Epidemiology and Genetics, National Cancer Institute, National Institutes of Health, Rockville, Maryland*

ARTICLE INFO

Article history:
Received 29 May 2024
Revised 4 March 2025
Accepted 1 April 2025
Available online 9 April 2025

Keywords:
cervical cancer
human papillomavirus
metaplasia
reserve cell
thin high-grade squamous intraepithelial lesion
transformation zone

ABSTRACT

Squamous cervical cancers generally arise as a result of persistent infection with high-risk human papillomaviruses (hrHPVs) and occur near the squamocolumnar junction (SCJ) and within the transformation zone (TZ). The susceptibility of the TZ to HPV-related carcinogenesis appears linked to epithelial cell plasticity, with squamous metaplasia originating from a specialized stem cell population at this site. Two alternative cell populations have been implicated: keratin (K)7+ve cuboidal cells located at the SCJ vs a more broadly distributed K17+ve cervical reserve cell population. To distinguish between the hypotheses, we utilized multiplex immunofluorescence and large-scale digital imaging to map cell populations at the TZ of 165 women with and without hrHPV infections. Our results did not reveal a distinct population of K7+ cuboidal cells at the SCJ but found instead that the cuboidal and columnar cells of the TZ express K7 and K8 throughout and lack the p63 transcription factor required for epithelial stratification. Squamous metaplasia and reserve cells, which are defined by their subcolumnar location and pattern of biomarker expression (K5/K17/P63), were conspicuous at cervical crypt entrances within the TZ extending proximally toward the endocervix. In HPV-infected tissue, crypt-entrance regions with thin high-grade squamous intraepithelial lesion pathology showed prominent expression of hrHPV E6/E7 mRNA, as detected by fluorescence in situ hybridization, and p16/MCM expression, with infection also apparent in neighboring reserve cells. In some instances, normal/uninfected reserve cells (E6/E7 mRNA−ve) and squamous metaplasia were not only seen close to these regions of hrHPV infection but also extended well beyond the infected area both laterally and by depth. Our results confirm that the reserve cells underneath the columnar epithelia at TZ have the potential to undergo malignant squamous transformation via reserve cell proliferation, in agreement with previous histopathological studies. These translational findings highlight the importance of understanding the molecular biology of the epithelial sites where HPV cancers develop and suggest that in high-risk individuals, treatment strategies should target a wider area than previously thought.

* Corresponding authors.
E-mail addresses: desanjose.silvia@gmail.com (S. de Sanjosé), schiffmm@exchange.nih.gov (M. Schiffman), jd121@cam.ac.uk (J. Doorbar).

https://doi.org/10.1016/j.labinv.2025.104166

Introduction

Cervical cancer is the fourth most common cancer in women, with more than half a million cases diagnosed annually worldwide.[1-3] Over 95% of these cancers[4] are caused by persistent infections with "high-risk" human papillomaviruses (hrHPVs), the most common sexually transmissible agents. In mature squamous epithelium, they typically cause low-grade intraepithelial lesions (LSILs) controlled by the immune system.[5] However, persisting infection can lead to the development of high-grade squamous intraepithelial lesions (HSILs) (-) or high-grade cervical intraepithelial neoplasia (designated as CIN3 or more equivocally, CIN2),[6,7] which are the precursors of cervical cancer treated upon detection during standard screening procedures.[8] Although the World Health Organization term HSIL is broadly equivalent to the alternative classification of CIN2/3, the term "thin HSIL" is used to describe lesions that are <10 cells thick, and which are thought to develop directly from infected (proliferating) reserve cells or immature squamous epithelium. HSIL/CIN3 originating from the thicker mature glycogenated squamous epithelium appears to arise from a preceding LSIL, with the 2 pathways of cancer progression suggested as a result of different sites within the cervix. The treatment of precancerous cervical lesions includes loop electrosurgical excision procedure (LEEP) or cryo-/thermal ablation.[9]

The vulnerability of the uterine cervix to hrHPV infection and neoplastic progression is linked to its unusual epithelial architecture, with most cervical cancers arising within the transformation zone (TZ).[10] The cervical TZ is the region between the original stratified squamous epithelium of the ectocervix and the simple columnar epithelium of the endocervix.[10] The TZ is a site of epithelial cell plasticity that undergoes metaplasia, a normal physiological process in which one epithelial type is replaced by another as a response to hormonal and environmental changes.[11] As observed by Smedts et al,[12] keratin expression changes during squamous metaplasia, with reserve cells and metaplastic cells acquiring keratins typical of squamous differentiation, highlighting the plasticity and differentiation potential within the TZ. Although metaplasia at the cervical TZ can occur throughout life, there are several key periods where it has been well documented, coinciding with fetal development, adolescence, and pregnancy.[13-15] During these times, hormonal changes and alterations in the tissue microenvironment drive the transformation of columnar epithelium into stratified squamous epithelium.[13,16,17] At puberty and thereafter, the columnar epithelium of the TZ is gradually replaced by a thicker, protective stratified squamous epithelium. This process is mediated by local changes in the tissue microenvironment, female hormones, and exposure to the acid environment of the vagina (a byproduct of normal lactobacillus metabolism), which may cause inflammation.[11] As a result, the location of the squamocolumnar junction (SCJ) moves within the TZ, with its position generally visible colposcopically as a boundary between the pink squamous epithelium and the bright red region, which marks the thinner columnar epithelium of the TZ and ectocervix. The TZ is defined by colposcopists, as the region between the original and current SCJ where metaplasia has already occurred, and is bounded by the last region of metaplasia.[13,18] Reich et al[13] have proposed an additional "extended TZ" definition that includes the region lying immediately proximal (higher up into the canal) where there is potential for subsequent metaplasia. In this area, reserve cells are distributed throughout the entire tall columnar endocervical epithelium including the endocervical canal. The SCJ is—as the name implies—is the junction or border between 2 different types of epithelia.

Despite the importance of cervical TZ in the development of cervical cancer, most HPV research has centered around the molecular biology of hrHPV as the causal agent.[19] It is clear from these studies that hrHPV targets important regulators of epithelial homeostasis to modulate proliferation, differentiation, and intercellular signaling,[20,21] and that HSIL arises when these viral mechanisms become deregulated.[21] It is unclear why the TZ is a hot spot for hrHPV carcinogenesis, with current models linking the site's vulnerability to not only an increased risk of infection but also to the unusual epithelial plasticity of the TZ region and the deregulated hrHPV gene expression.[11] Previous studies have pointed to the existence of sporadically distributed p63-positive cells located between the columnar cells and the basal lamina of the TZ,[22] suggesting that these cells are the cervical reserve cells described by pathologists many decades ago.[23] It has been suggested that these cells may be the target cells for hrHPV infection at the cervix.[18,22] However, other target cells have been prominently proposed, including a cuboidal cell type that, unlike the cervical reserve cell, has been reported to be found at the SCJ.[17]

In this study, we applied multiplex immunofluorescence and digital imaging techniques to map the distribution of cell types and their involvement in epithelial stratification within the cervical TZ, utilizing biopsies collected from 165 women with and without hrHPV infections. We explored the distribution of these cells in relation to the original and current SCJ, as well as the cervical crypts, which extend from the surface of the TZ into the underlying stroma. In addition to p63, we used several keratin-based biomarkers to determine cell identity and lineage. These studies, which initially focused on uninfected/normal tissue, were subsequently extended to cervical tissue infected by hrHPV and treated for HSILs. Our observations provide a framework on which to develop an understanding of in vivo HPV cancer susceptibility, with implications relating to disease recurrence and treatment strategies in susceptible/high-risk groups.

Materials and Methods

Collection and Processing of Clinical Samples

The biopsy material used in this study included excisional specimens from individuals who underwent LEEP for HPV-associated cervical precancer at the Hospital de Clinic, Barcelona, Spain (aged between 23 and 63 years; 18 cases), and National Health Laboratory Services, Johannesburg, South Africa (aged between 33 and 58 years; 30 cases). Ethical approval was obtained from the institutional review boards of both institutions. Additional clinical material was drawn from archival sources described in previous publications,[24,25] including hysterectomy-derived histologically normal cervical specimens (aged between 30 and 85 years; 117 cases). Patient data for all the samples were anonymized. Formalin-fixed paraffin-embedded blocks were sectioned (32 × 5 μm) onto Klinipath Frost Printer microscope slides (VWR International B.V.) and processed for immunohistochemical and whole tissue section-PCR analysis.[26] Conditions for PCR-clean sectioning have been described previously.[24,25] HPV genotyping was carried out by SPF_{10}-PCR-DEIA-$LiPA_{25}$, version 1 (Labo Biomedical Products BV[27]) or using the Atila Biosystems AmpFire HPV High-Risk Genotyping system (GHPVF-100[28]).

Table
Antibodies used for fluorescent immunohistochemical staining

Target	Supplier, location	Cat. no.	Dilution	Host	Amplification	Target/interpretation
Cytokeratin 17 (K17)	Abcam, Cambridge	ab51056	1/400	Rabbit	Yes	Reserve cell at the SCJ or within the TZ. Variably present in metaplasia
Cytokeratin 5 (K5)	Abcam, Cambridge	ab52635	1/100	Rabbit	No	Reserve cell at the TZ, ectocervical basal cell
p63	Abcam, Cambridge	ab735	1/100	Mouse	Yes	Reserve cell at the TZ, ectocervical basal cell
Cytokeratin 7 (K7)	Abcam, Cambridge	ab181598	1/100	Rabbit	No	Columnar cells at the SCJ, TZ, and endocervix Variably present in reserve cells
Cytokeratin 8 (K8)	Abcam, Cambridge	ab53280	1/100	Rabbit	No	Columnar cells at the SCJ, TZ, and endocervix
Cytokeratin 13 (K13)	Abcam, Cambridge	ab92551	1/100	Rabbit	Yes	Cells of the stratified epithelium
p16	Roche/Ventana, Tucson, USA	MTM-E 6H4	1/200	Mouse	Yes	Deregulated hrHPV E6/E7 expression (when used with MCM)
MCM	Cell Signalling Technology, USA	3619	1/400	Rabbit	Yes	Deregulated hrHPV E6/E7 expression (when used with p16)
HPV E4	Pan-specific E4 mAb (prepared in-house)	FH1.1	1:25	Mouse	Yes	Productive stages of the HPV life cycle
HPV L1	Native Antigen, UK	MAB12279	1:100	Mouse	Yes	Productive stages of the HPV life cycle

HPV, human papillomavirus; hr, high risk; SCJ, squamocolumnar junction; TZ, transformation zone.

Morphologic Examination of Clinical Samples and Disease Pathology

Hematoxylin and eosin (H&E)–stained, brightfield scanned images were captured using a Pannoramic MIDI automatic digital slide scanner (3DHISTECH). The diagnosis of LSIL, HSIL, and the characterization of cell types were carried out by a panel of 3 pathologists (J.O., T.O., and H.G.) at Hospital de Clinic, Barcelona, National Health Laboratory Services, Johannesburg, South Africa, and Cambridge, using the captured scans as described previously[24,25] according to standard morphologic criteria.[29] HPV-associated lesions were graded according to the Lower Anogenital Terminology Standardization criteria, with references to mitotic figures, koilocytes, nuclear/cytoplasmic ratio, loss of epithelial maturation, and the involvement of cervical crypts in TZ. Recent studies have shown that p16 positivity in squamous metaplasia can indicate transcriptionally active hrHPV, even in the absence of dysplastic morphologic features, supporting the utility of p16 as an early biomarker in HPV-associated HSIL.[30]

Regions showing no HPV-associated pathology, with an uninfected appearance, were classified as “normal.”

Immunofluorescent Staining and Detection of Human Papillomavirus RNA

Fluorescent immunohistochemistry was performed as described previously[24] using the basic set of markers listed later. Rabbit anti-K17, anti-K5, and mouse anti-p63 antibodies were used to detect reserve cells,[22] while anti-K13 was used to detect cells undergoing epithelial stratification. Columnar cells in the TZ and endocervix were detected using rabbit anti-K7 and anti-K8. The HPV E4 protein was detected using the pan-specific mouse E4 monoclonal antibody (FH1.1[24]; Table).

The RNAscope 2.0 assay system was used for the detection of hrHPV E6/E7 mRNA (Advanced Cell Diagnostics, Inc), with development using Tyramide-Plus fluorescein, diluted 1/1500 in dilution buffer at 40 °C for 30 minutes (Perkin Elmer, NEL 760001KT; catalog number: 311521) before DAPI counterstain. Positive cases had prominent granular cytoplasmic (and nuclear) staining when compared with negative control tissue. RNA integrity and suitability for HPV transcriptional analysis were confirmed in each tissue section using the control probe Pol2A, which detects housekeeping gene expression (catalog number: 310451). HPV-positive and -negative organotypic rafts were used as controls for the expression of E6/E7.

Fluorescent Image Capture and Image Analysis

Immunofluorescence images were captured using either a Pannoramic MIDI automatic digital slide scanner, a Zeiss laser scanning confocal 700 microscope, or a Zeiss Axiovision microscope, depending on the sample being analyzed. Images were subsequently analyzed using the ZEN 3.5 Image Analysis software (Zeiss Microscopy), SlideViewer (3DHISTECH), and Adobe Photoshop (Adobe Systems). Measurements of the TZ from the original SCJ to either the current SCJ, the last area of metaplasia, or the last reserve cell,[13,17] including crypt depth from the epithelial surface, were carried out using the linear measurement annotation tool on the SlideViewer (3DHISTECH). In HPV-infected tissue, measurement was made to the last area of LSIL/HSIL. Tissue section slides stained for viral mRNA were imaged on a Zeiss laser scanning confocal microscope 700 (version 1.1), equipped with an argon laser and He/Ne 633 nm laser.[31]

Statistical Evaluation of Immunofluorescence Data

Data obtained from the measurements across the TZ including the extended TZ and depths of crypts were compiled in Microsoft Excel, where average values and SDs were calculated to summarize the measurements. Statistical significance between measurement groups including the HPV-infected and -uninfected biopsies was determined to identify differences in TZ and crypt depth metrics, supporting comparative analyses of metaplastic progression and HPV infection impact.

Results

Distribution and Diversity of Epithelial Cell Types at the Cervical Transformation Zone

The key histologic features of the cervical TZ and the endocervix in H&E-stained tissues are shown in Figure 1A, B. The TZ and endocervix, unlike the ectocervix, have a highly invaginated surface, with numerous secretory crypts lined with a single layer

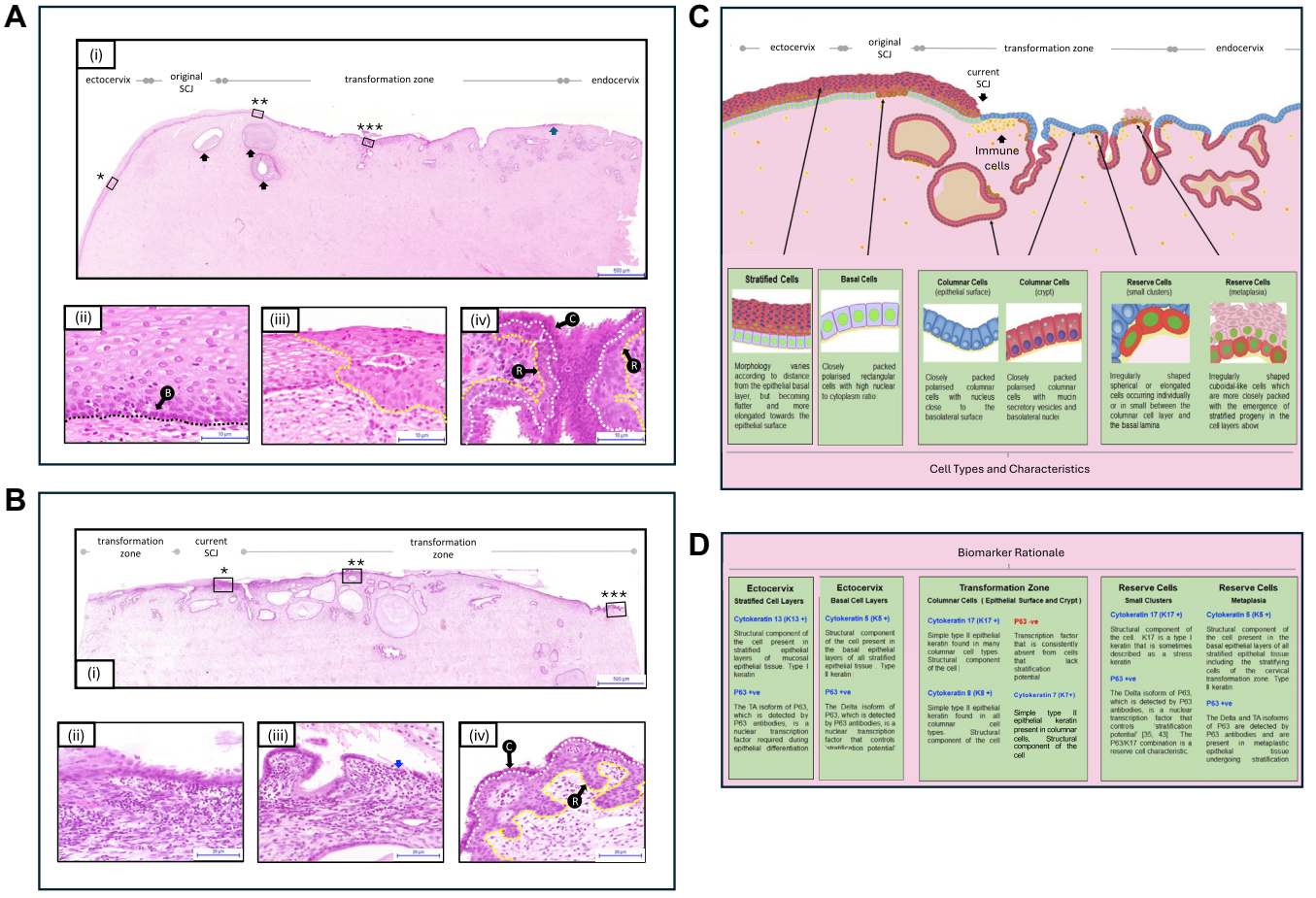

Figure 1.

Characterization of epithelial cells at the cervical transformation zone. (A) (i) Brightfield scan of an hematoxylin and eosin (H&E)-stained normal cervix (case: 14-) illustrating the epithelial cell types found at the ectocervix (left), the endocervix (right), and the cervical transformation zone (TZ) adjacent to the original squamo-columnar junction (SCJ) (scale bar = 500 μm). Enlargements of the highlighted regions (*), (**), and (***) in (A) are shown in (ii), (iii), and (iv). (A[ii]) The basal cells (arrow labeled "B") form a closely packed layer beneath the stratified cell layers of the ectocervix. The position of the basal lamina is indicated by a black dotted line (scale bar = 10 μm). (A[iii]) Metaplasia adjacent to the current SCJ is delineated at the right of the image by the yellow dotted line (scale bar = 10 μm). (A[iv]) Cervical crypt entrance showing columnar cells (arrow labeled "C"), which are being sloughed off following reserve cell (arrow labeled "R") expansion. Approximate boundaries between the stromal, reserve, and columnar cell layers are marked by the yellow and white dotted lines (scale bar = 10 μm). The "last" region of metaplasia (blue arrow), which marks the conventional boundary of the TZ, is indicated in the low-power image shown in (A[i]). (B[i]) Brightfield scan of H&E-stained normal cervical TZ showing metaplasia adjacent to the "current SCJ" (case: 6-) (scale bar = 500 μm). Enlargements of highlighted regions (*), (**), and (***) are shown in (ii), (iii), and (iv). (B[ii]) Current SCJ with adjacent metaplasia (scale bar = 20 μm). (B[iii]) The cells that cover the surface epithelium of the TZ are heterogeneous and exhibit both cuboidal (blue arrow) and columnar appearances (scale bar = 20 μm). (B[iv]) Region of active immature metaplasia with reserve cells (arrow labeled "R") forming a metaplastic epithelium underneath an intact layer of columnar/cuboidal cells (arrow labeled "C") (scale bar = 20 μm). The white dotted line indicates the boundary between the 2 cell types. (C) Schematic representation of key features of the normal cervix, which comprises the ectocervix, the TZ, and the endocervix. Long arrows show the location of the different cell types examined in this study, with boxes indicating morphologic features of the different cell types present in the cervical epithelium. (D) The molecular phenotypes of the cell types are outlined in the boxes. From the left, the stratified epithelium of the ectocervix expresses K5/p63 in the basal and parabasal layers and K13 in the suprabasal cells. Arrows within the TZ highlight columnar cells, which express K17 and 8 but not p63. The 2 rightmost arrows highlight reserve cells at the TZ, which express K17 and p63.

of columnar epithelial cells. We defined the TZ as the region between the original SCJ and the last (most proximal) area of metaplasia[13] (blue arrow in Fig. 1A). The TZ shows a range of unique morphologic features, including immature and mature metaplasia and the presence of cervical reserve cells, often associated with metaplasia and displaced columnar epithelial cells (Fig. 1A-C). Although the hysterectomy patient age range in our cohort spanned more than 31 years, with the youngest (age 23 years; Supplementary Table S1) being well beyond puberty, metaplasia was apparent in all the biopsies examined, which agrees with our understanding that metaplasia is a dynamic process that occurs throughout a woman's life.[32] It was also apparent from our analysis that metaplasia is not confined to the immediate vicinity of the SCJ, but as shown in Figure 1A, is distributed widely at sites that appear quite distant from SCJ. Multifocal or irregular SCJ regions were often apparent in these lesions, particularly at crypt entrance sites where metaplasia and an increased density of stromal immune cells were observed (Figs. 1A, B, and 2).

Discrimination Between Current Models of Cervical Metaplasia using Molecular Biomarkers

Although subcolumnar reserve cells were conspicuous in H&E-stained TZ tissue (Fig. 1A, B), we aimed to define the cell types

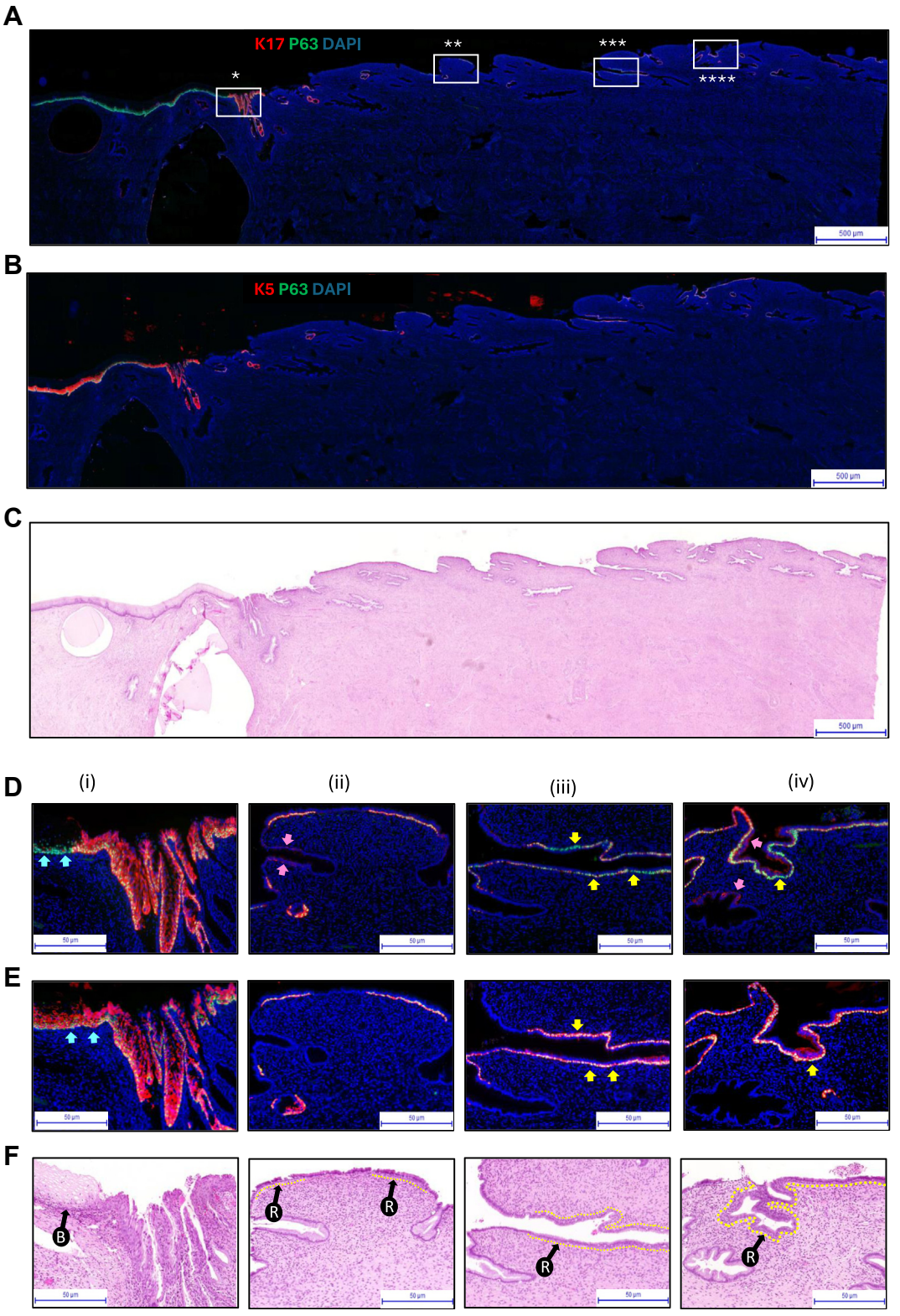

Figure 2.
Molecular phenotype and location of reserve cells in the transformation zone (TZ). (A) Immunofluorescence scan of normal cervix stained for p63 (green) and K17 (red), counterstained with DAPI (case: 3−) (scale bar = 500 µm). Enlargements of the highlighted regions marked (*), (**), (**), and (****) are shown in (D). (B) Adjacent tissue section stained for p63 and K5 counterstained with DAPI (scale bar = 500 µm). Enlargements of the highlighted boxes are shown in (E). (C) Hematoxylin and eosin–stained brightfield scan of subsequent tissue section from the same sample (scale bar = 500 µm). Enlargements of the highlighted boxes are shown in (F). D[i] Magnification of the current squamocolumnar junction (SCJ). Reserve cells undergoing metaplasia strongly express K17 throughout every layer, although expressing p63 in the basal and parabasal layers. Basal cells at the SCJ do not express K17 but express p63 in the basal and parabasal layers (turquoise arrows) (scale bar = 50 µm). (D[ii-iii]). Magnification of reserve cells lining cervical crypt entrances, emphasizing the heterogeneity of their K17 and p63 expression (scale bar = 50 µm). In (D[iv]), the pink arrows point to intermittent K17 columnar cells,

present at the cervix using cell-specific molecular markers (Fig. 1D). Two distinct models have been proposed to explain the process of metaplasia at the TZ. The "reserve cell model" suggests the importance of the K17/p63-positive subcolumnar reserve cells,[33,34] whereas the "cuboidal cell model" proposes the involvement of K7-positive cuboidal cells located in a narrow band at the SCJ.[17] Although the simple epithelial cells at the SCJ were sometimes squatter, with a cuboidal appearance in places (Fig. 1B and Supplementary Fig. S1), we observed significant cellular morphologic heterogeneity at the SCJ and the presence of cuboidal cells outside the SCJ (Supplementary Fig. S1). In many cases, the simple epithelial cells adjacent to the SCJ were rounded and/or poorly polarized and formed part of a locally disorganized epithelial structure. In contrast to what has been reported,[17] we could not identify a unique population of cytokeratin 7 (K7)-positive cells (cuboidal or otherwise) at the SCJ. Instead, we found that K7 was expressed by columnar cells lining cervical crypts and the surface of TZ and endocervix, which we confirmed by the presence of K8, a marker for differentiated simple epithelia[31] (Supplementary Figs. S1 and S2).[35,36]

We next looked at K17, which has been reported to be a marker of cervical reserve cells[22] (Fig. 3D). To distinguish these cells from columnar cells, an additional marker, p63, was used (Fig. 1D).[37] Reserve cells were highlighted by the K17/p63 biomarker pair and were apparent as "strings" of cells lying immediately beneath the K7/K8-positive columnar cells at multiple locations across the cervical TZ (Fig. 3D and enlargements in [i-ii]). The association of reserve cells with crypt entrances and their immediate vicinity was apparent in many of the biopsies examined (Fig. 3D, K). Interestingly, the remnants of cervical crypts (including associated reserve cells) remain beneath the stratified epithelium of the TZ, even after metaplasia is complete (Fig. 3K). Although both reserve cells and the basal layer of the stratified epithelium of the TZ express p63, the expression of K17 declines during the process of metaplasia, and the stratified epithelium of the TZ becomes indistinguishable from that of the ectocervix (Fig. 2). Indeed, K17, a "stress keratin" transiently expressed during wound healing,[38-40] was generally absent in mature stratified epithelium (Fig. 2A). K5, a well-characterized basal cell marker, was present in both basal and reserve cells and typically showed a more uniform and robust expression than K17 (Fig. 3E, L). Interestingly, in the stratified epithelium of the TZ, K5 staining extended into the residual crypt entrances where the K17-positive reserve cells were found, with K5-positive basal cells of the TZ being continuous with the K5/K17-positive cells present at the crypt entrances (Fig. 3D, E, K, and L). These K5/K17/p63-positive cells were variably positive for the simple epithelial cell marker K8 (Fig. 3J[i]) and (less conspicuously) K7 (Fig. 3H[iv]). When taken together, our studies support the hypothesis[10,41,42] that reserve cells give rise to the stratified epithelium of the cervical TZ during metaplasia, with the stratification potential of these cells making them a plausible cellular target for infection by HPV.

Defining Molecular and Histologic Characteristics of Reserve Cells

The aforementioned observations confirm that reserve cells can be identified by their unique expression of cytoplasmic K17 and nuclear p63. However, we identified a K17-reserve cell population expressing the "basal cell" marker K5 (Fig. 2A–D) and seemingly increased expression of p63 compared with K17-positive reserve cells and basal cells (Fig. 2A, B, D, and E). Although basal cells and reserve cells share a common biomarker pattern, K17 seems to be transiently expressed only in reserve cells.[39,43] P63 was found in both basal and reserve cells, reflecting its role as a regulator of squamous epithelial differentiation. Interestingly, previous studies[18,34] have suggested a distinction between the K17/p63 reserve cell, which we found also to express K5, and which has a progenitor function for squamous metaplasia, and the K5/p63/K7 reserve cell, which may serve as the progenitor for glandular renewal.[18,34] Our findings suggest that the latter reserve cell population might be in a later stage of differentiation, often expressing low levels of K8 in addition to K7, and indeed, K7 and K8 were often detected in reserve cells at low levels (Fig. 3H, J). This may correspond to the results reported by Fritsch et al[16] who identified 2 distinct reserve cell lineages: p63/CK17-positive (squamous epithelium precursors) and CK7-positive (columnar epithelium precursors) reserve cells at the TZ. K5/K17 dual positivity is apparent in cells at the SCJ (Fig. 2A, B[i]), with K17 absent in the mature stratified epithelium of the TZ SCJ (Fig. 2D[i]). K5, on the other hand, was present in cells undergoing metaplasia as well as in the stratified cells of the TZ (Fig. 2D [i]-F). In summary, we defined the molecular phenotype of cervical reserve cells as always K5/p63 positive, often K17 positive, and variably K7/K8 positive. In addition, we defined the proliferating reserve cells histologically as a "string" of rounded cells lying beneath the columnar cells of the TZ. Interestingly, metaplasia gives rise to intermediate morphologies, including K17-positive/p63-negative columnar cells located close to areas of reserve cell expansion (Fig. 2D[ii, iv]), supporting the idea that K17 can be transiently expressed in both the squamous and columnar cell lineages.[44] A timeline from reserve cell expansion to a fully differentiated stratified epithelium is outlined in Supplementary Figures 2 and 3.

We established the average crypt depth within the cervical TZ and found that crypt depth generally increases in the region between the original and current SCJ (Supplementary Table S1). A fraction of cervical crypts harbor reserve cells, which present no significant difference in their depths, with a consistent average depth of 0.8 mm (Supplementary Table S1). Reserve cells were distributed widely throughout the cervical TZ and extended well beyond the region where the last metaplasia occurred; this may be referred to as an "extended TZ," which is referred to as the area where squamous metaplasia may potentially occur.[13] On average, reserve cells extend 8 mm beyond the area of the last metaplasia. As this region has the potential to undergo metaplasia, it appears that the boundary between the TZ and the endocervix is inaccurate.[13]

whereas in (D[iii]), the yellow arrows point to reserve cells with low K17 and high p63 expression. (D[iv]) Magnification of reserve cells lining the surface epithelium and cervical crypts, with heterogeneity of K17 and p63 expression, pointed out by pink/yellow arrows (scale bar = 50 μm). (E[i]) Magnification of the SCJ (scale bar = 50 μm). Reserve cells undergoing metaplasia strongly express K5 throughout every layer, although expressing p63 at the basal and parabasal layers. Basal cells at the SCJ also strongly express K5 and p63 in the basal and parabasal layers (turquoise arrows). (Eii, iii) Magnification of reserve cells lining cervical crypt entrances, which homogenously and stably express K5 (scale bar = 50 μm). In (E[iii]), yellow arrows indicate the uniform appearance of p63/K5 reserve cells in a crypt. (E[iv]) Magnification of reserve cells lining the surface epithelium and cervical crypts expressing K5 (scale bar = 50 μm). Hematoxylin and eosin stain of (F[i]) SCJ, the basal cells (arrow labeled "B") at the stratified epithelium of the TZ. (F[ii, iii]) reserve cells (arrows labeled "R") lining cervical crypt entrances, separated from the basal lamina by a yellow dotted line, and (F[iv]) reserve cells (arrows labeled "R") at the surface of the epithelium and lining the cervical crypt, separated from the basal lamina by a yellow dotted line (scale bar = 50 μm).

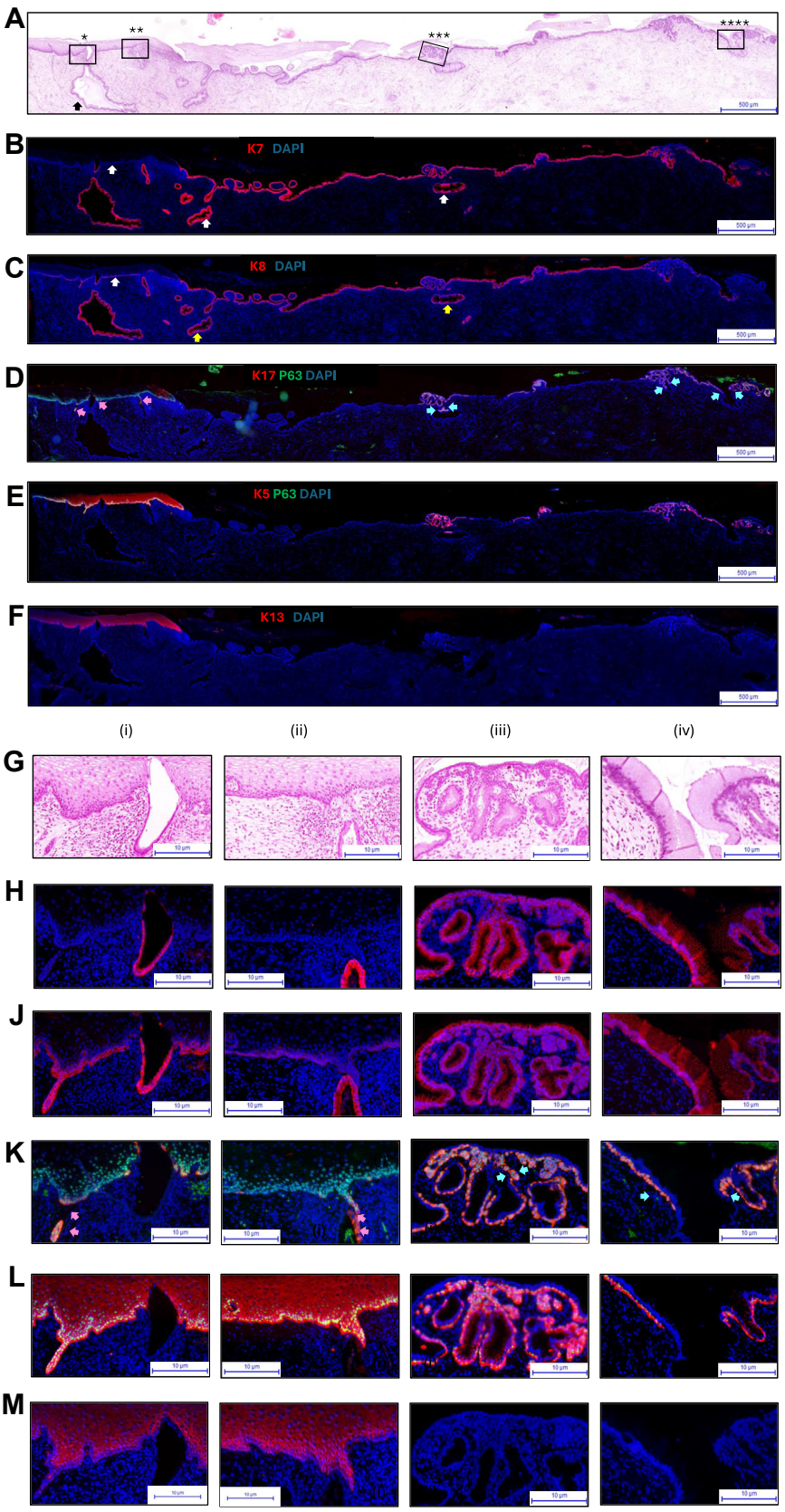

Figure 3.

Cell metaplasia is defined by K5/K17/p63 positivity and histologic characteristics. Images show (case: 7-). (A) Brightfield scan of hematoxylin and eosin–stained normal cervix (scale bar = 500 μm). (B) Tissue section stained for K7 (red), counterstained with DAPI (blue) (scale bar = 500 μm). (C) Tissue section stained for K8 (red), counterstained with DAPI (scale bar = 500 μm). (D) Tissue section stained for p63 (green) and K17 (red), counterstained with DAPI (scale bar = 500 μm). Turquoise arrows highlight crypts and crypt entrances. (E) Tissue section stained for p63 and K5 (red), counterstained with DAPI (scale bar = 500 μm). (F) Tissue section stained for K13 (red), counterstained with DAPI (scale bar = 500 μm). Crypt filled with mucin (black arrow) is indicated in the low-power image shown in (A). White and yellow arrows show the hierarchical appearance of K7/K8 expression in columnar

Reserve Cells as Targets for Human Papillomavirus–Induced HSIL at the Transformation Zone

We next sought evidence that reserve cells are involved in the development of HPV-associated precancers.[18,22,42] One hundred sixty-five LEEP biopsies were collected from women who had been treated for HSIL. After staining for p16, MCM, and E4, a subset was selected for staining with the cell-specific markers outlined in Figure 1D.[24,45] As reported previously, p16/MCM are coexpressed at full epithelial thickness in HSIL,[24] whereas in LSIL, p16/MCM (when expressed) occur in the lower/middle layers, with E4 and L1 marking life cycle completion.[25] Figure 4 (H&E shown in 4A[i]) shows an E4-negative p16/MCM-positive HSIL adjacent to an area of immature metaplasia (Figs. 2 and 3). K17/p63 reserve cells were prominent in immature metaplasia (Fig. 4B-D) and appeared to extend continuously into the region where HSIL was found (Fig. 4B [iii and iv]). This continuity between K17-positive reserve and basal cells was frequently seen in HSIL (including thin HSIL) at the crypt entrance (Figs. 4B[ii], C[i] and 5). These regions were characterized by displaced columnar cells, as seen during reserve cell metaplasia (Fig. 4C[i]). Heterogeneity in p16/MCM staining in basal and reserve cells was apparent within these "transitional regions" (Fig. 4B[i]-D[i]), with the level of basal cell K17 (but not K5) declining away from the metaplasia/HSIL junction (Fig. 4C, D). The thin variant of HSIL was also observed at the crypt entrance (yellow dotted lines in Fig. 5B[i, iii]) and sometimes was seen to extend into the crypt.[46]

Reserve cells were found adjacent to crypt-associated thin HSIL (Supplementary Table S2), occurring either continuously with neoplastic basal cells or as isolated cells (Fig. 5). When compared with uninfected cervical tissue, the crypts in the HPV-infected women were typically distended and mucus filled and penetrated much deeper into the stromal layers (Fig. 5A). The significantly increased crypt depth is associated with an increased reserve cell depth (Supplementary Table S2), which may have implications for treatment.

Human Papillomavirus Infection of Epithelial Sites Within the Cervical Transformation Zone

As cervical reserve cells can predominate at the entrances to the cervical crypts, we next wondered whether infections at this site were apparent in situations where there was no overlying p63-positive squamous epithelial tissue. The LEEP specimen shown in Figure 6 shows the cross-sectional anatomy of the cervix, including the central os, ectocervix, original SCJ, and the multiple crypt entrances and crypt structures between (Figs. 6 and 7 and Supplementary Fig. S4). Widespread HPV16-associated HSIL was present throughout the TZ, bounded on each side by the ectocervix and endocervix. As expected, the ectocervix was characterized by the prominent expression of p63 (along with K5), but as a mature nonmetaplastic epithelium, did not express K17. K13 is a marker of epithelial stratification at this site[47] and was found throughout the differentiating epithelial layers of the ectocervix but not the epithelial basal cells. Curiously, the epithelium covering the TZ did not express the usual markers of epithelial stratification (ie, K13, p63, or K5) but instead expressed the simple epithelial cell markers, K7 and K8 (Fig. 6F, G). In marked contrast to this, the cervical crypt entrances stained with antibodies to p16/MCM (which suggests deregulated HPV E6/E7 expression) and were marked by the prominent expression of p63 and K17. Such lesions are typically designated as thin HSIL and are characterized by 9 or fewer cell layers and are associated with p16 overexpression.[46] Similar to what is shown in Figure 5, p63/K5-positive cells, which in this case were p16/MCM and HPV RNA positive, were sometimes detected beneath the columnar cells of the deeper crypt with the characteristic phenotypic behavior of reserve cells (Fig. 7B[iii]; yellow arrows). Although the extensive K17/p63 distribution at the crypt entrance resembles that seen in metaplasia, the lesions were not undergoing conventional epithelial stratification and did not support K13 expression (Fig. 7 and Supplementary Fig. S4), despite the progressive decline in p63. When taken together, our results suggest that the crypt entrance region and the expanding K5/K17/p63 reserve cell population, which localize to this region, are important targets for HPV infection.

Reserve Cells Harbor Abortive Human Papillomavirus Infection

Although p16/MCM is considered a unique biomarker of deregulated HPV E6/E7 expression in HSIL, we used an RNAscope in situ approach to directly confirm HPV deregulation at crypt entrances. A conspicuous E6/E7 gene expression pattern was apparent in the K5/K17/p63 reserve cells at crypt entrances (Fig. 7A[iv] and Supplementary Fig. S4). Interestingly, viral gene expression declined sharply toward the epithelial surface, probably as cells divide and leave the crypt entrances. The surface epithelial cells of the TZ were p63− and K7/K8+ and marked an upper boundary of the crypt entrance (Fig. 7A[vi, vii] and Supplementary Fig. S4). The loss of the E6/E7 RNAscope signal was also apparent within the body of the crypt, which appeared to mark the lower boundary of HPV gene expression. In some crypts, the sporadic occurrence of individual E6/E7-expressing cells beneath crypt-lining columnar cells could be observed (Fig. 7A[vi, vii], and 7B), in line with the sporadic p16/MCM positivity among the K5/K17/p63 reserve cell found at this location. Interestingly, the columnar cells in the crypts were occasionally p16 positive in the vicinity of these sporadic HPV-positive reserve cells (yellow arrows, Fig. 7). Deregulated HPV gene expression at crypt entrances, as suggested by p16 and E6/E7 expression, was observed in 13 LEEP biopsies that were analyzed further in Supplementary Table S2. The average distance from the original SCJ to the last HSIL (Fig. 8 and Supplementary Table S2) is 10.9 mm, which is similar to the distance between the original SCJ to the last metaplasia seen in the uninfected tissue (13.57 mm; distance 2B [TZ] in Fig. 8 and Supplementary Table S1) but shorter than the distance between the original SCJ and the last identifiable reserve cell (21.30 mm; distance 2A [extended TZ], Fig. 8 and Supplementary Table S1),

cells in (B) and (C). The remnants of K17 reserve cells underneath the stratified epithelium of the transformation zone (TZ) (pink arrows) and clusters of p63/K17 reserve cells at the entrance of crypts (turquoise arrows) are indicated in the low-power image shown in (D). (G[i-iv]) Magnifications of regions highlighted in (A) (boxes [*], [**], [***], and [****]) (scale bar = 10 μm). (G[i, ii]) Cervical crypt entrance underneath the newly formed stratified epithelium. (G[iii]) Multiple layers of reserve cells underneath a single layer of cuboidal columnar cells. (G[iv]) Single layer of reserve cells underneath elongated columnar cells. (H[i-iv]) Magnifications of regions highlighted in (A) stained for K7, counterstained for DAPI (scale bar = 10 μm). (J[i-iv]) Magnifications of regions highlighted in (A) stained for K8, counterstained with DAPI (scale bar = 10 μm). (K[i-iv]) Magnifications of regions highlighted in (A) stained for p63 and K17, counterstained with DAPI (scale bar = 10 μm). The pink and turquoise arrows highlight the features described in panel D as mentioned above. (L[i-iv]) Magnifications of regions highlighted in (A) stained for p63 and K5, counterstained with DAPI (scale bar = 10 μm). (M[i-iv]) Magnifications of regions highlighted in (A) stained for K13, counterstained with DAPI (scale bar = 10 μm).

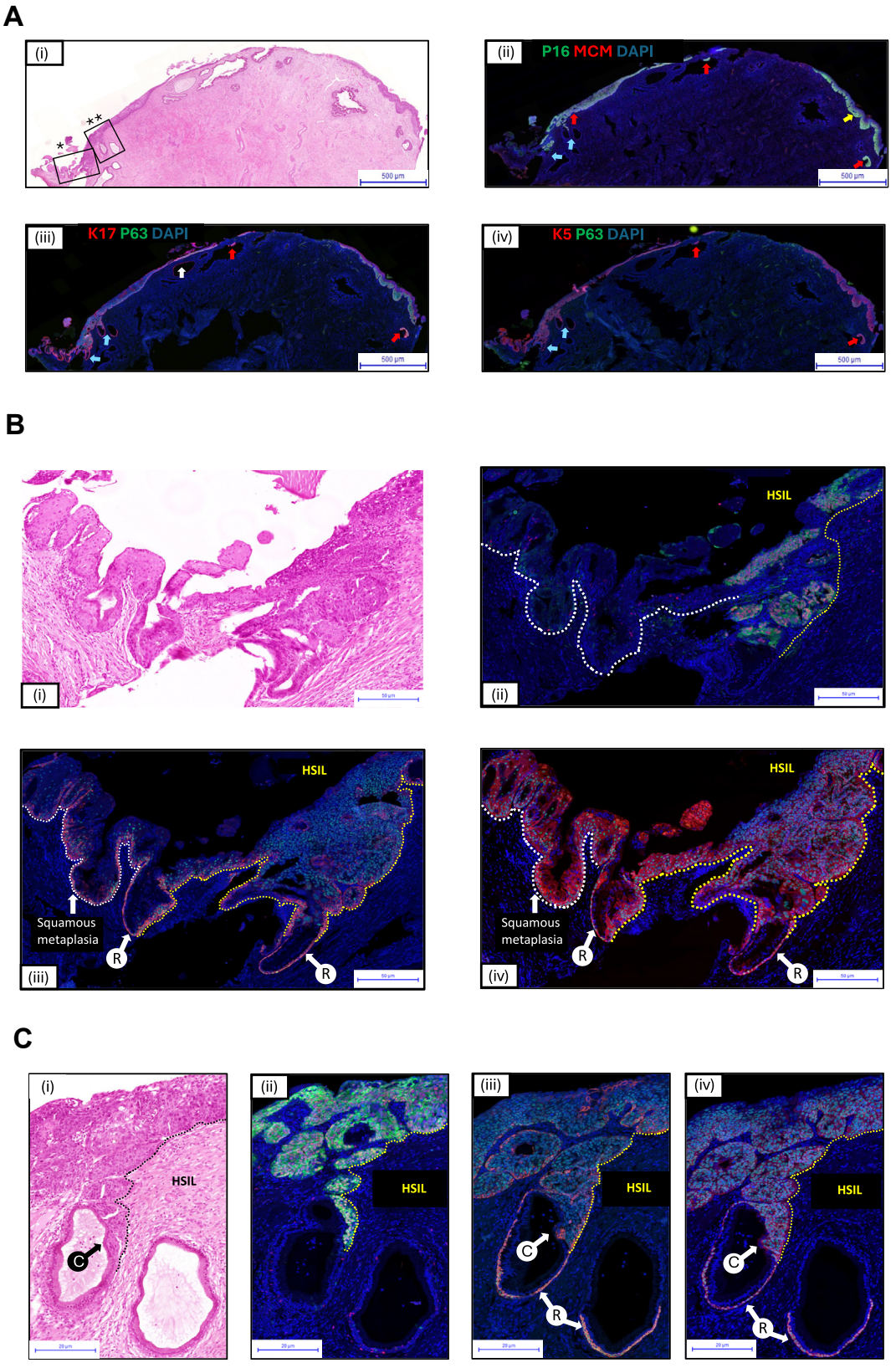

Figure 4.

Human papillomavirus–associated intraepithelial neoplasia and its association with the cervical reserve cell population. (A[i]) Brightfield scan of hematoxylin and eosin–stained human papillomavirus–infected high-grade squamous intraepithelial lesion (HSIL) (CIN3) section. (Case: 1+ [Supplementary Table S2]) (scale bar = 500 μm). (A[ii]) Adjacent section stained for p16 and MCM counterstained with DAPI. (A[iii]) Adjacent tissue section stained for p63 and K17, counterstained with DAPI (scale bar = 500 μm). (A[iv]) Subsequent tissue section from the same sample stained for p63 and K5, counterstained with DAPI (scale bar = 500 μm). Red/yellow arrows point to neoplastic regions, turquoise arrows point to adjacent noninfected reserve cells in images, and white arrow points to K17 intermittent columnar cells (ii-iv) (scale bar = 500 μm). Magnifications of the boxed

which suggests that the standard LEEP procedure may not always eliminate the reserve cell population. Curiously, the region where metaplasia was found was similar to the region where HSIL (usually thin HSIL) was seen in the infected tissue, extending 13.57 mm and 10.87 mm from the original SCJ, respectively (Fig. 8). The average number of crypts containing reserve cells was lower in the infected samples than in the uninfected samples, which may reflect that the normal reserve cell population has been replaced by a proliferating cell population.

Discussion

It is well established that the majority of squamous cell cervical precancers arise in the metaplastic epithelium of the cervical TZ.[10,18,48] Using multiplex immunostaining technology and digital imaging, we provide further insight into the role of reserve cells in cervical carcinogenesis. Our observations suggest that at the level of biomarker detection, the p63-positive reserve cells are not restricted to the cervical SCJ. Instead, they are dispersed more widely across the TZ (Fig. 4) and can become prominent following reserve cell expansion, which we noticed can center around the entrances to the cervical crypts, and which has potential implications for the treatment and recurrence of cervical precancers.[13,49] This aligns with previous findings,[50,51] which emphasized that squamous cell carcinomas in the cervix may sometimes arise from reserve cells underlying the endocervical columnar epithelium rather than the stratified squamous epithelium.[52] Reserve cells appear to be a central determinant of cervical TZ biology and carcinogenesis, with Fritsch et al suggesting that their presence in vaginal and cervical epithelium arises from the urogenital sinus during fetal development.[16,53] By late fetal life and in newborns, these cells are said to be restricted to the region of the TZ and the adjacent cervical epithelium.[18] Other models of reserve cell presence have also been proposed,[54] although the term reserve cell is not always applied[17] or is used inconsistently.[55] Interestingly, from our analysis, cervical reserve cells typically appear singly and as short, disconnected groups beneath the columnar cell monolayer and strongly express the "defining markers" K17, K5, and p63. A timeline that involves reserve cell expansion around the entrances to the cervical crypts is suggested, followed by subsequent maturation into a differentiated stratified epithelium to create new SCJs.[13,28]

HPVs are intracellular parasites that utilize the biosynthetic machinery of the host cells to establish a reservoir of infection that allows viral genome maintenance.[56] To achieve this, the viral E6 and E7 proteins modulate cell differentiation, cell density, and proliferation,[48,57] with deregulated E6/E7 expression driving the development of intraepithelial neoplasia. The analysis of clinical biopsies, when linked to our understanding of HPV biology, provides new insights into the HPV-driven carcinogenic process that have been difficult to establish using tissue culture or animal models alone. This analysis has been further facilitated, by recent advances in tissue-based protein and mRNA detection methodologies, and in computer-based digital imaging and image analysis approaches. Using cervical tissue from uninfected hysterectomy biopsies, we have characterized the spatial distribution and biomarker profile of reserve cells in the absence of infection. This builds on previous studies that highlighted the metaplastic potential of the subcolumnar reserve cells and suggested their potential role in the development of cervical neoplasia.[22,50,51,58,59] Reserve cells, which are first evident as single, disconnected strings of cells, appear to increase in number and expand gradually under the columnar cell layers without showing signs of differentiation (Supplementary Figs. S2 and S3). Although their subcolumnar localization clearly marks them apart from the ectocervical basal cells, reserve cells expressed both K5 (a well-established basal cell keratin marker that is involved in cell adhesion and mechanical strength) and p63, which is essential for keratinocyte stratification. The variability in K17 staining was not reported previously[22] but most likely reflects the pleiotropic roles of K17 as a "stress keratin"[38-40] (Figs. 1, 2D, E, and 3A-D). These results are broadly in line with the idea that reserve cells and basal cells perform a stem cell function at the cervix,[33] with the microenvironment determining the cells' identity and role in epithelial homeostasis.[33] Although the columnar cells of the TZ lack K17 and p63 (Fig. 2B, C, H[iii-iv], and J[iii-iv]), they all express K7/K8 to a greater or lesser extent depending on location. Curiously, and in line with other recent reports,[16,33] we did not observe a discrete population of cuboidal cells, distinguished by the expression of K7 at the SCJ. In our hands, K7 expression was widespread across the cervical TZ, although a hierarchy of staining was noticeable, in line with the idea that increasing K8 expression marks a population of more differentiated columnar cells.[36] Reserve cells were widely distributed within the TZ, supporting the observation that metaplasia is not restricted to the SCJ but occurs throughout the TZ, with the columnar epithelium at the crypt entrances forming an important region where this occurs. Reserve cells appear to initiate the process of metaplasia and build a stratified epithelium, which is thought to result from local "irritation" or inflammation, which can occur throughout a woman's lifetime, following cervical/vaginal pH changes, at puberty or during pregnancy.[10,60]

Our results suggest that the presence and distribution of reserve cells could be used to better define the cervical TZ, as these cells can undergo squamous metaplasia when conditions allow.[18] Interestingly, it also appears from our work that reserve cells typically extend 20 mm or more beyond the original SCJ (Fig. 8), extending beyond the last region of metaplasia. In the tissues examined, the average distance between the original SCJ and last reserve cell was 20.79 mm, whereas between the new SCJ and last reserve cell, the average distance was 16.69 mm (distance A and [A-C] in Fig. 8). Because of the limited size of the tissue available to us, we were not able to determine how far reserve cells persisted into the endocervical canal. Moreover, among the LEEP biopsies examined here, the excised HSILs typically extended to only 10 mm. It was also noted that crypt depth was increased in HPV-associated HSILs, and that when present, the reserve cells could be found in association with these deep crypts. These results suggest that the reserve cell pool may not always be eradicated by the standard LEEP procedure, although this process is often an effective strategy for the treatment of HSILs. It would appear that the remaining reserve cells, which we anticipate are capable of squamous metaplasia, may persist as targets for HPV infection and contribute to the ongoing risk of HSIL, especially in individuals who cannot effectively control or clear their infection. Reich and

regions marked (*) and (**) highlighted in (A) are shown in (B[i-iv]) and (C[i-iv]), respectively. (B[i-iv]) Magnification of neoplastic region adjacent to the area of immature metaplasia. White and yellow dotted lines mark the basal lamina. Arrows labeled R point to noninfected reserve cells near the neoplastic regions (scale bar = 50 μm). (C[i])-(D[iv]) Magnification of neoplastic region at the cervical crypt entrance. Black and yellow dotted lines trace the basal lamina. Arrows labeled R point to uninfected reserve cells near the neoplastic regions, whereas arrows labeled C point to columnar cells lining the infected crypt and undergoing displacement by the underlying HSIL (scale bar = 20 μm).

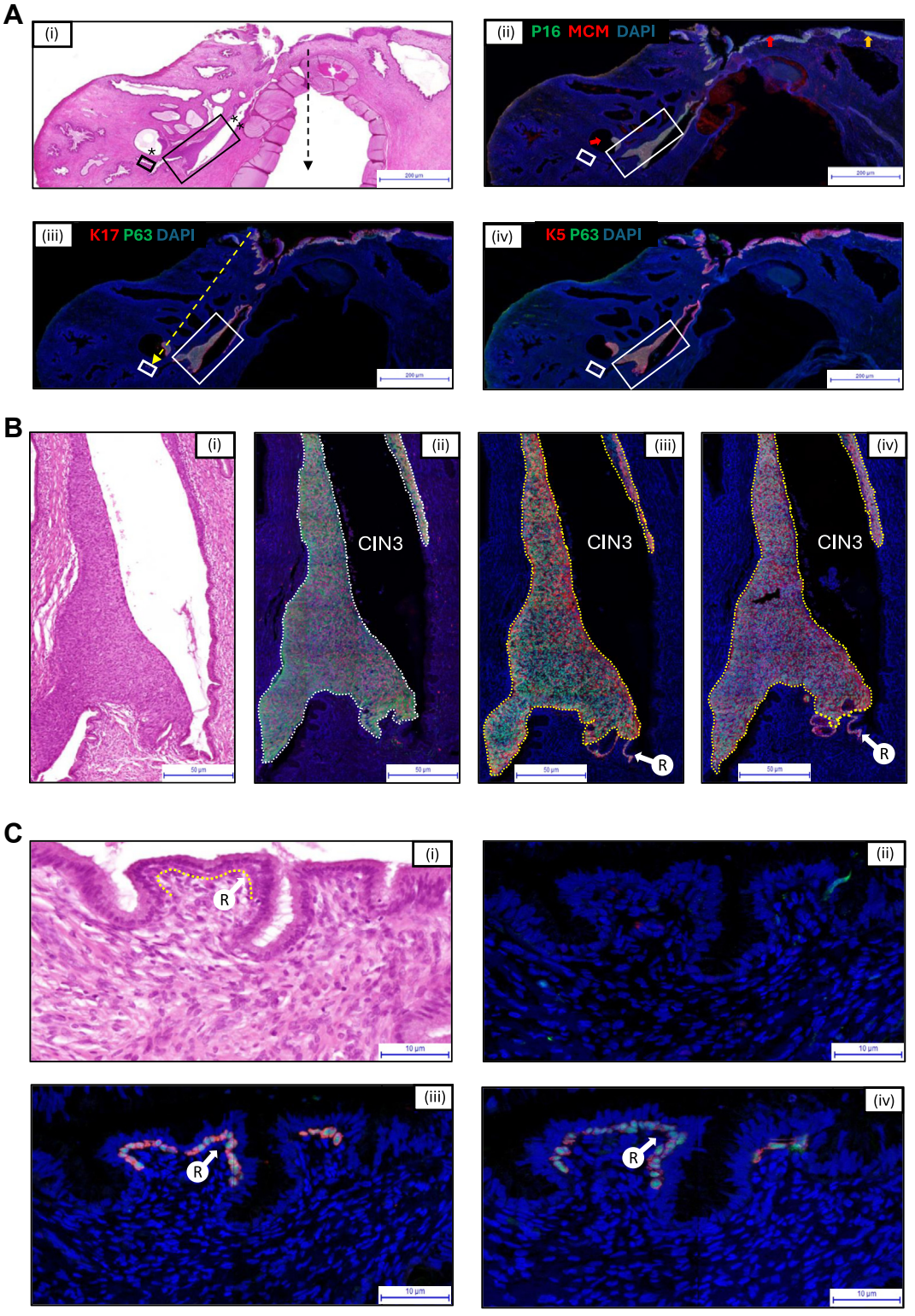

Figure 5.

Reserve cells can occur deep in the crypts and be continuous with areas of high-grade squamous intraepithelial lesion (HSIL). (A[i]) Brightfield scan of hematoxylin–eosin–stained human papillomavirus–infected tissue section from an HSIL (CIN3) lesion. The black dotted arrow marks an enlarged crypt (case: 9+) (scale bar = 200 μm). (A[ii]) Adjacent tissue section from the same sample stained for p16 and MCM and counterstained with DAPI (scale bar = 200 μm). Red arrows identify HSIL (CIN3) areas, whereas yellow arrows point to HSIL (CIN2). (A[iii]) Adjacent tissue section stained for p63 and K17. The yellow dotted arrow indicates a region where uninfected reserve cells are apparent in a deeper crypt. (A[iv]) Adjacent section from the same sample stained for p63 and K5. Sections are counterstained with DAPI. Scale bar = 200 μm. Magnifications of the boxed regions marked (*) and (**) highlighted in (A) are shown in (B[i-iv]) and (C[i-iv]), respectively. (B[i-iv]) HSIL and thin HSIL within a cervical crypt. Arrows labeled "R" point to reserve cells adjacent to the neoplastic region (scale bar = 50 μm). (C[i-iv]) Reserve cells lining a deep cervical crypt. Arrows labeled "R" point to isolated, uninfected reserve cells. The basal lamina is traced by a dotted line in (A[ii]). Scale bar = 10 μm.

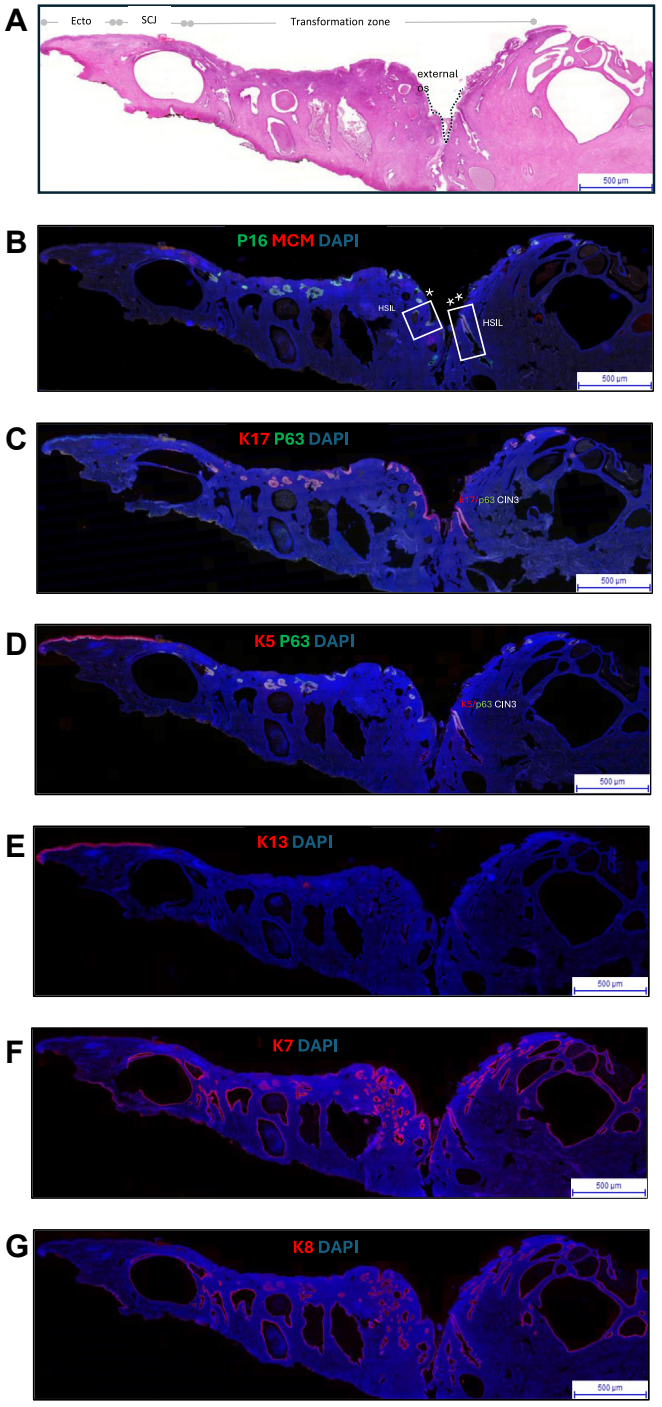

Figure 6.
Human papillomavirus infection of the reserve cell region within the cervical transformation zone. (A) Brightfield scan of hematoxylin and eosin-stained human papillomavirus–infected high-grade squamous intraepithelial lesion (CIN3) tissue section (case: 5+). Adjacent sections are shown in subsequent panels following staining with (B) p16 and MCM. (C) p63 and K17, (D) p63 and K5, (E) K13, (F) K7, and (G) K8. The 2 high-grade squamous intraepithelial lesion regions are marked (*) and (**) and are shown at higher magnification in Figure 7 and Supplementary Figure S4. All sections are counterstained with DAPI. Scale bar = 500 µm. SCJ, squamocolumnar junction.

Regauer[50] proposed that targeting these reserve cells in therapeutic strategies could reduce the recurrence of HSIL or progression to invasive squamous cell carcinoma by eliminating potential HPV reservoirs in high-risk individuals. Effective surgical or ablative treatment is required to minimize recurrence risk, with this being particularly important in individuals with immune deficiency, eg, women living with HIV, particularly in low-resource settings where surveillance for recurrence is not practicable.[61] Although cuboidal cells were sometimes present at the SCJ,[17] we did not consistently identify such cells (Fig. 1B and Supplementary Fig. S1A, E). Indeed, cells with cuboidal and other atypical appearances were detected at other sites in the TZ, often in association with elevated stromal immune cell activity (Fig. 1 and Supplementary Fig. S1). As described previously, we did not observe that cells adjacent to the SCJ were uniquely K7 positive (Supplementary Fig. S1 and Fig. 2B), a finding that has also been reported by others.[16,33]

The stimulation and proliferation of reserve cells is typically independent of HPV infection, with the driving forces including pH change, inflammation, and mechanical irritation. When HPV infection of already proliferating reserve cells occurs, it is thought that this proliferative stimulus is boosted, leading to the possibility of cellular transformation. Although this process may be initiated at all sites where reserve cells reside, it is thought to occur initially at the surface epithelium first, where stimuli for metaplastic metaplasia first reach reserve cells and where initial contact with HPV is achieved. Here we show that HPV infection of the cervical TZ can lead to an expansion of the subcolumnar K5/K17/p63 reserve cell population at the entrance to the cervical crypts, with HSILs (typically thin HSIL) developing at these sites in association with a prominent expression of the HPV E6/E7 proteins (Fig. 7 and Supplementary Fig. S4) focally at the SCJ.[17] Indeed, we postulate that the expanding K5/K17/p63 reserve cells at the crypt entrance may represent a stem cell region where the balance between self-renewal and reserve cell differentiation is regulated. This region is likely to be a dynamic environment where external signals influence cell behavior via the regulation of gene expression, including that of the infecting HPV.[62] We also evaluated the distribution of cervical crypts across the TZ and endocervix in uninfected cervical biopsies (Supplementary Tables S1 and S2 and Fig. 8), which is important given that the LEEP procedure typically aims to excise to a level of ~4 mm below the surface of the cervix. Crypts located underneath the stratified epithelium of the TZ were often mucin filled and enlarged due to crypt entrance blockage (Figs. 1A and 3A; Nabothian cysts). Interestingly, the crypts appearing in the HPV-infected biopsies were larger and deeper than those seen in uninfected women, which may also reflect the obstruction of the crypt entrances by regions of HSIL. The total number and average depth of crypts lined by reserve cells may be linked to the chance of finding reserve cells post-treatment and is an important consideration given that the ablation of susceptible cells has been suggested as a strategy to prevent the development of HSIL.[17,18] Our results show that subcolumnar reserve cell numbers generally decrease in deeper crypt regions when compared with regions closer to the epithelial surface and the crypt entrances. How LEEP affects subsequent reserve cell distribution, and future susceptibility to infection and neoplasia, remains to be established.

Several molecular markers, including p16, MCM, and E4, were used alongside cellular biomarkers and tissue morphologic analysis (Fig. 1), to distinguish between productive and abortive HPV infections. The p16/MCM distribution supported a role for reserve cells in the development of HSIL, including thin HSIL, which has been proposed to represent a distinct pathway to cervical carcinogenesis.[46] As an adjunct to p16/MCM staining, direct evidence of HPV infection and gene expression was sought using an RNAscope approach, a novel in situ hybridization technique that

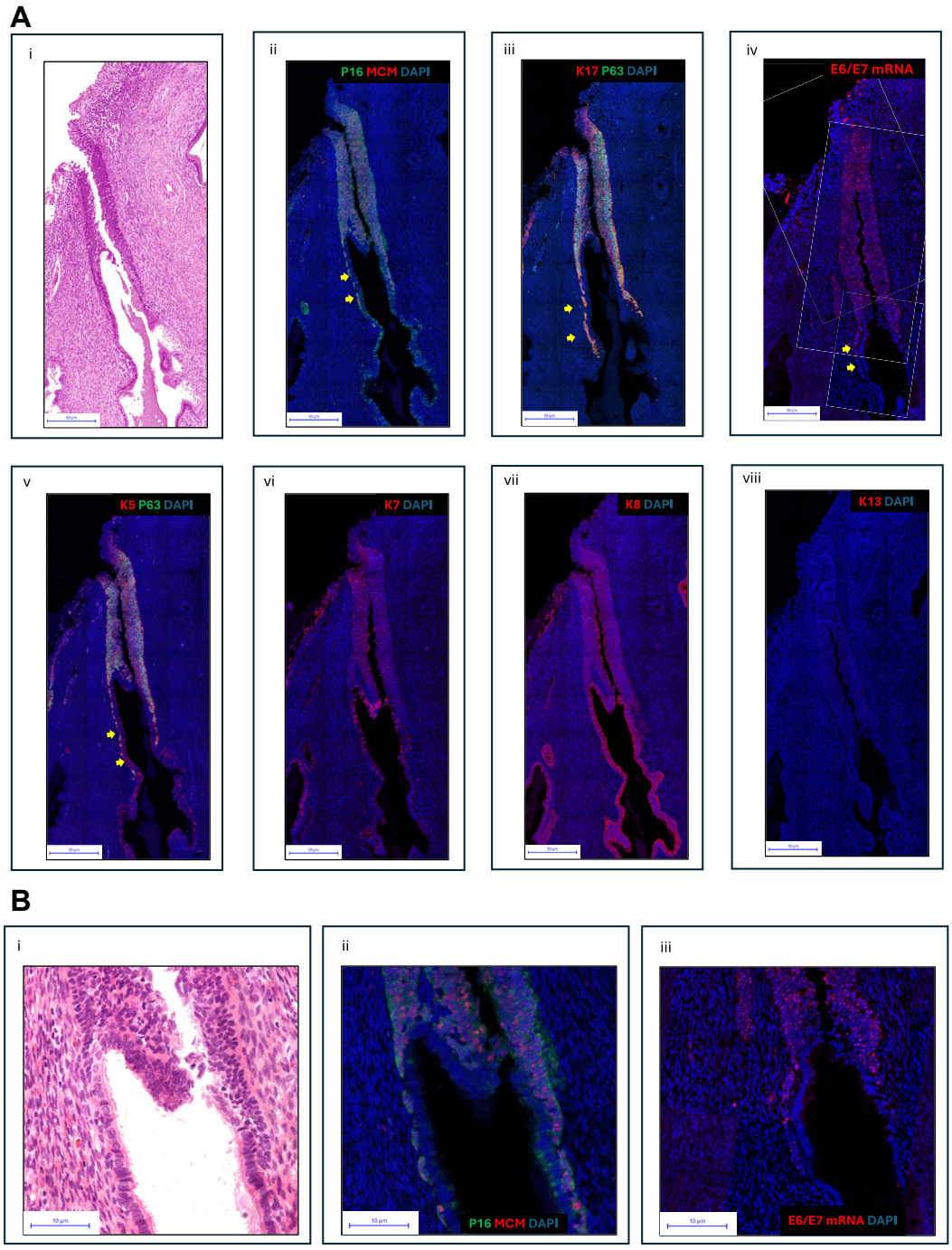

Figure 7.
Characterization of human papillomavirus (HPV) infections at crypt entrances using viral and cellular biomarkers. (A[i]) Brightfield scan of hematoxylin and eosin–stained HPV-infected high-grade squamous intraepithelial lesion (CIN3) section (case: 5+ [Supplementary Table S2]) (scale bar = 50 μm). Adjacent sections are shown in the panels below and are stained for (ii) p16 and MCM, (iii) p63 and K17, (iv) high-risk HPV E6/E7 mRNA (RNAscope), (v) p63 and K5, (vi) K7, (vii) K8, and (viii) K13. All sections are counterstained with DAPI. Yellow arrows in (ii)-(v) point to reserve cells adjacent to the neoplastic region. Scale bar = 50 μm. (B[i-iii]) Magnification of HPV mRNA at crypt entrances and in columnar reserve cells. Scale bar = 10 μm.

allows the direct detection of HPV mRNA expression. Even in mixed lesions with different HPV-associated pathologies, the crypt entrances stood out as sites where the E6/E7 gene was particularly highly expressed, with strong RNAscope signals correlating with p16/MCM positivity (Fig. 7 and Supplementary Fig. S4). The possibility that the basal cells of the ectocervix and the crypt-entrance reserve cells of the TZ may control viral gene expression differently appears reasonable and is suggested by our RNAscope analysis (Fig. 7 and Supplementary Fig. S4), with the local cellular microenvironment most probably contributing to the process. Interestingly, the E6/E7 levels sometimes declined toward the epithelial surface, and when analyzed using the molecular markers described in Figure 3, the overlying surface cells at the TZ lacked P63 but expressed K7/K8. The absence of an E6/E7

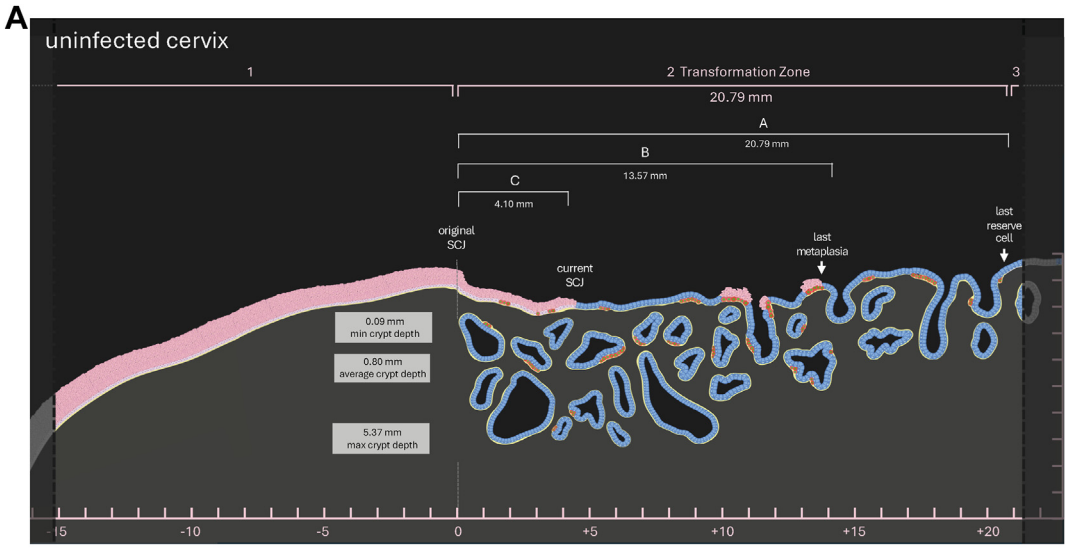

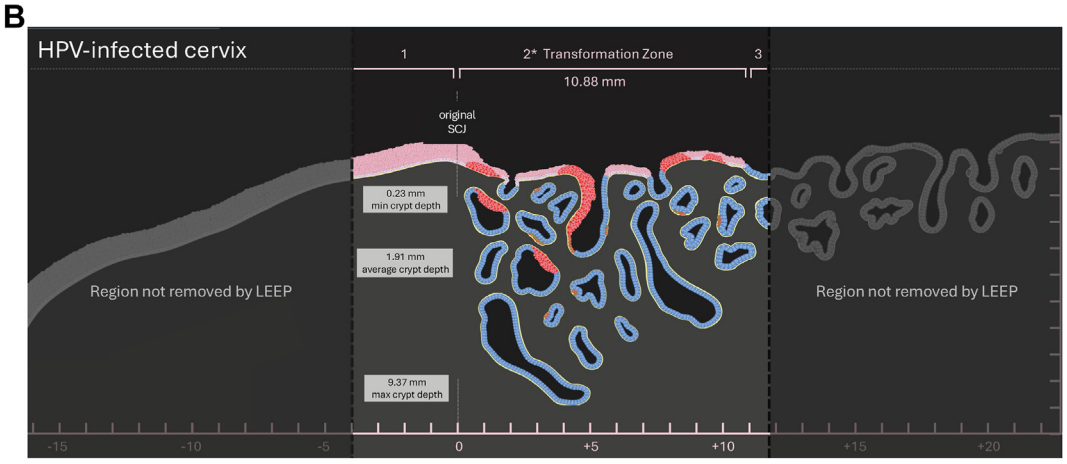

C

2A: Region from original SCJ to last reserve cell 2B: Region from original SCJ to last metaplasia 2*: Region from original SCJ to last neoplasia		Uninfected Cervix (hysterectomy-derived) HPV Negative N = 15	HPV Infected Cervix (LLETZ-derived) HPV Positive N = 15	T-test	
Average Length of Region 1 (mm)		15.2	4.0	Not applicable	
2A versus 2*	Average Length of TZ (mm)	20.79	10.88	P < 0.01	P = 9.357e-8
	2A versus 2* - Average Number of Crypts per mm	2.29	2.55	Not significant	P = 0.6
	2A versus 2* - Average Depth of Crypts	0.88	1.88	P < 0.01	P = 0.0003
	2A versus 2* - Average Proportion of Crypts with RC	0.29	0.04	P < 0.01	P = 4.9e-5
	2A versus 2* - Average Depth of Crypts with RC	0.75	2.68 (4 observations)	Not significant	P = 0.22
2B versus 2*	Average Length of TZ (mm)	13.57	10.88	Not significant	P = 0.08
	2B versus 2* - Average Number of Crypts per mm	1.88	2.55	Not significant	P = 0.17
	2B versus 2* - Average Depth of Crypts	0.91	1.88	P < 0.01	P = 0.0006
	2B versus 2* - Average Proportion of Crypts with RC	0.32	0.04	P < 0.01	P = 0.00015
	2B versus 2* - Average Depth of Crypts with RC	0.73 (13 obvs)	2.68 (4 observations)	Not significant	P =0.22
Average Length of Region 3 (mm)		0.36	0.88	Not applicable	

Figure 8.
Comparative analysis of key features between the infected and uninfected cervix. (A) Feature locations and measurements derived from uninfected cervical epithelium as outlined in Supplementary Table S1. Biopsies obtained from hysterectomy specimens typically extended >2 cm into the transformation zone (TZ) (from the original squamocolumnar junction [SCJ] and encompassed both the last metaplasia and the reserve cells beyond (extended TZ). The position of the original SCJ (between region 1 and region 2) represents a common reference point from which comparative measurements have been made. Axes at the bottom and right of the image show distances in millimeters from the original SCJ. (B) Location of features and measurements from human papillomavirus–infected biopsies collected after loop electrosurgical excision procedure (LEEP). Biopsies obtained by LEEP typically extended <2 cm into the TZ (from the original SCJ), as indicated by the boxed area, with regions not removed during the LEEP shown to either side. (C) Comparison of the TZ in the uninfected cervix (2A and 2B) with the TZ region present in LEEP biopsies from HPV-infected women (2*). 2B corresponds to the conventional definition of the TZ, whereas 2A corresponds to the "extended TZ," which spans the region from the original SCJ to the last detected reserve cell. Rows highlighted in green/blue compare the uninfected and infected cervical transformation zones, with particular emphasis on the distribution of reserve cells and their depth in infected and uninfected tissue. Rows highlighted in gray reveal differences in the size of the biopsies, which were more limited in the samples collected by LEEP.

RNAscope signal within the body of the crypt beneath the crypt entrance suggests a restriction on HPV gene expression that may restrict lesion expansion.

Reserve cells are identified as p63/K17-positive progenitor cells located beneath the columnar epithelium, with the capability to undergo squamous metaplasia. Recent research by Fritsch et al[16] suggests that the distribution of these cells during postnatal and adult stages is determined prenatally. Our study has confirmed previous findings that reserve cells, rather than the overlying columnar epithelium or K7 SCJ cells, are the primary precursors for metaplastic transformation and the initiation of HPV-associated neoplastic processes. The idea that reserve cells may under some circumstances be generated de novo[54] cannot be excluded, given that K5-positive/p63-positive cells can be generated from columnar epithelium at other sites.[63,64] Because reserve cells already express key markers associated with epithelial stratification, their intrinsic plasticity likely facilitates the rapid transition from metaplasia to neoplasia under oncogenic pressure. A deeper understanding of these processes could enhance our approach to cervical cancer prevention, particularly in defining treatment margins for ablative therapies aimed at eliminating high-risk precursor populations.

Understanding the biology and dynamics within the TZ is pivotal to understanding the pathogenesis of HSIL. The TZ, per pathology, refers to columnar epithelium that has differentiated into immature and mature squamous epithelium, with the latter being distinguished from the ectocervix by the presence of underlying crypts. By contrast, colposcopists define the TZ as the region extending from the original SCJ to the current SCJ, where squamous metaplasia has occurred.[13] However, from the treatment of cervical precancer and prevention of recurrence perspective, TZ should be defined as an area where squamous metaplasia has occurred or is likely to (re)occur.[13] Based on the findings in this article, this may include the region, both proximally and in-depth, where the last reserve cell, as well as the last HPV infection, is located rather than the visible current SCJ or even the region where the last area of metaplasia is already apparent (Supplementary Table S3). When taken together, our results suggest that the presence of susceptible cells in underlying crypts, and beyond the last region of metaplasia, may sometimes contribute to the risk of post-treatment recurrence, even in instances where the more evident lesional margins are clear.

Acknowledgments

The authors thank Michael Chung (Emory University) and Chemtai Mungo (University of North Carolina) for their comments and insights during the preparation of the manuscript.

Author Contributions

M.S., J.D., S.d.S., and H.G. contributed to funding and project conceptualization. A.A., H.G., and K.S. carried out the experiments and established protocols. A.A., H.G., K.S., T.O., J.O., H.K., M.d.P., K.D., S.d.S., M.S., and J.D. made data interpretation, experimental design, and project direction. T.O., J.O., and H.G. made pathology interpretation. C.W. contributed to data visualization. All authors read and approved the final version of the paper.

Data Availability

Raw data measurements pertaining to reserve cell distributions are provided in the supplementary tables that accompany this manuscript.

Funding

The study was funded by the National Cancer Institute Intramural Research Program with a supplemental award from the Office of AIDS Research. Additional funding was provided by the Medical Research Council (MR/S024409/1) and the Cambridge Trust.

Declaration of Competing Interest

None reported.

Ethics Approval and Consent to Participate

Ethical approval was provided from the Review Boards of Hospital de Clinic, Barcelona, Spain, and the National Health Laboratory Services, Johannesburg, South Africa.

Supplementary Material

The online version contains supplementary material available at https://doi.org/10.1016/j.labinv.2025.104166

References

1. Singh D, Vignat J, Lorenzoni V, et al. Global estimates of incidence and mortality of cervical cancer in 2020: a baseline analysis of the WHO Global Cervical Cancer Elimination Initiative. *Lancet Glob Health*. 2023;11(2):e197–e206. https://doi.org/10.1016/S2214-109X(22)00501-0
2. Bray F, Ferlay J, Soerjomataram I, Siegel RL, Torre LA, Jemal A. Global cancer statistics 2018: GLOBOCAN estimates of incidence and mortality worldwide for 36 cancers in 185 countries. *CA Cancer J Clin*. 2018;68(6):394–424. https://doi.org/10.3322/caac.21492
3. Crosbie EJ, Einstein MH, Franceschi S, Kitchener HC. Human papillomavirus and cervical cancer. *Lancet*. 2013;382(9895):889–899. https://doi.org/10.1016/S0140-6736(13)60022-7
4. Doorbar J, Quint W, Banks L, et al. The biology and life-cycle of human papillomaviruses. *Vaccine*. 2012;30(Suppl 5):F55–F70. https://doi.org/10.1016/j.vaccine.2012.06.083
5. Mishra GA, Pimple SA, Shastri SS. An overview of prevention and early detection of cervical cancers. *Indian J Med Paediatr Oncol*. 2011;32(3):125–132. https://doi.org/10.4103/0971-5851.92808
6. Schiffman MH. New epidemiology of human papillomavirus infection and cervical neoplasia. *J Natl Cancer Inst*. 1995;87(18):1345–1347. https://doi.org/10.1093/jnci/87.18.1345
7. Schiffman M, Doorbar J, Wentzensen N, et al. Carcinogenic human papillomavirus infection. *Nat Rev Dis Primers*. 2016;2:16086. https://doi.org/10.1038/nrdp.2016.86
8. Crum CP, Meserve EE, Peters IIIWA. Cervical squamous neoplasia. In: *Diagnostic Gynecologic and Obstetric Pathology*. Elsevier; 2018:298–374.
9. Kyrgiou M, Athanasiou A, Paraskevaidi M, et al. Adverse obstetric outcomes after local treatment for cervical preinvasive and early invasive disease according to cone depth: systematic review and meta-analysis. *BMJ*. 2016;354:i3633. https://doi.org/10.1136/bmj.i3633
10. Doorbar J, Griffin H. Refining our understanding of cervical neoplasia and its cellular origins. *Papillomavirus Res*. 2019;7:176–179. https://doi.org/10.1016/j.pvr.2019.04.005
11. Giroux V, Rustgi AK. Metaplasia: tissue injury adaptation and a precursor to the dysplasia–cancer sequence. *Nat Rev Cancer*. 2017;17(10):594–604. https://doi.org/10.1016/j.pvr.2019.04.005
12. Smedts F, Ramaekers F, Robben H, et al. Changing patterns of keratin expression during progression of cervical intraepithelial neoplasia. *Am J Pathol*. 1990;136(3):657–668.
13. Reich O, Regauer S, McCluggage WG, Bergeron C, Redman C. Defining the cervical transformation zone and squamocolumnar junction: can we reach a common colposcopic and histologic definition? *Int J Gynecol Pathol*. 2017;36(6):517–522. https://doi.org/10.1097/PGP.0000000000000381
14. Singer A, Reid BL, Coppleson M. A hypothesis: the role of a high-risk male in the etiology of cervical carcinoma: a correlation of epidemiology and molecular biology. *Am J Obstet Gynecol*. 1976;126(1):110–115. https://doi.org/10.1016/0002-9378(76)90474-9
15. Coppleson M. *Colposcopy : a scientific and practical approach to the cervix and vagina in health and disease. American lecture series no. 1020. American lectures*

in gynecology and obstetrics. Thomas; 1978:492. 2nd ed. xviii. ISBN-10: 0398037612; ISBN-13: 978-0398037611.
16. Fritsch H, Auer R, Hörmann R, Pechriggl E, Regauer S, Reich O. The development of the human vaginal fornix and the portio cervicis. *Clin Anat*. 2021;34(7):1059–1067. https://doi.org/10.1002/ca.23729
17. Herfs M, Yamamoto Y, Laury A, et al. A discrete population of squamocolumnar junction cells implicated in the pathogenesis of cervical cancer. *Proc Natl Acad Sci U S A*. 2012;109(26):10516–10521. https://doi.org/10.1073/pnas.1202684109
18. Regauer S, Reich O. The origin of human papillomavirus (HPV)-induced cervical squamous cancer. *Curr Opin Virol*. 2021;51:111–118. https://doi.org/10.1016/j.coviro.2021.09.012
19. Doorbar J, Jenkins D, Stoler MH, Bergeron C. Biology of the human papillomavirus life cycle: the basis for understanding the pathology of precancer and cancer. In: Jenkins D, Bosch FX, eds. *Human Papillomavirus*. Elsevier; 2020:67–83. https://doi.org/10.1016/B978-0-12-814457-2.00005-2
20. Scarth JA, Patterson MR, Morgan EL, Macdonald A. The human papillomavirus oncoproteins: a review of the host pathways targeted on the road to transformation. *J Gen Virol*. 2021;102(3):001540. https://doi.org/10.1099/jgv.0.001540
21. Medda A, Duca D, Chiocca S. Human papillomavirus and cellular pathways: hits and targets. *Pathogens*. 2021;10(3):262. https://doi.org/10.3390/pathogens10030262
22. Martens JE, Arends J, Van der Linden PJQ, De Boer BAG, Helmerhorst TJM. Cytokeratin 17 and p63 are markers of the HPV target cell, the cervical stem cell. *Anticancer Res*. 2004;24(2B):771–775. PMID:15161025.
23. Hellman L, Rosenthal AH, Kistner RW, Gordon R. Some factors influencing the proliferation of the reserve cells in the human cervix. *Am J Obstet Gynecol*. 1954;67(4):899–915. https://doi.org/10.1016/0002-9378(54)90110-6
24. Griffin H, Soneji Y, Van Baars R, et al. Stratification of HPV-induced cervical pathology using the virally encoded molecular marker E4 in combination with p16 or MCM. *Mod Pathol*. 2015;28(7):977–993. https://doi.org/10.1038/modpathol.2015.52
25. Griffin H, Wu Z, Marnane R, et al. E4 antibodies facilitate detection and type-assignment of active HPV infection in cervical disease. *PLoS One*. 2012;7(12):e49974. https://doi.org/10.1371/journal.pone.0049974
26. Quint W, Jenkins D, Molijn A, et al. One virus, one lesion—individual components of CIN lesions contain a specific HPV type. *J Pathol*. 2012;227(1):62–71. https://doi.org/10.1002/path.3970
27. Lall M, Dar L, Bhatla N, et al. Prevalence of human papillomavirus (HPV) genotypes in cervicovaginal secretions of human immunodeficiency virus (HIV) positive Indian women and correlation with clinico-virological parameters. *Front Reprod Health*. 2021;3:695254. https://doi.org/10.3389/frph.2021.695254
28. Tan Y-W, Lozano L, Chen X, et al. An isothermal, multiplex amplification assay for detection and genotyping of human papillomaviruses in formalin-fixed, paraffin-embedded tissues. *J Mol Diagn*. 2020;22(3):419–428. https://doi.org/10.1016/j.jmoldx.2019.12.004
29. Kurman RJ, Ellenson LH, Ronnett BM, eds. *Blaustein's Pathology of the Female Genital Tract*. 7th ed. Springer Science & Business Media; 2013.
30. Goyal A, Ellenson LH, Pirog EC. p16 Positive histologically bland squamous metaplasia of the cervix: what does it signify? *Am J Surg Pathol*. 2020;44(1):129–139. https://doi.org/10.1097/PAS.0000000000001364
31. Heddleston JM, Aaron JS, Khuon S, Chew TL. A guide to accurate reporting in digital image acquisition—can anyone replicate your microscopy data? *J Cell Sci*. 2021;134(6):jcs254144. https://doi.org/10.1242/jcs.254144
32. Reich O, Pickel H. 200 Years of diagnosis and treatment of cervical precancer. *Eur J Obstetr Gynecol Reprod Biol*. 2020;255:165–171. https://doi.org/10.1016/j.ejogrb.2020.10.037
33. Chumduri C, Gurumurthy RK, Berger H, et al. Opposing Wnt signals regulate cervical squamocolumnar homeostasis and emergence of metaplasia. *Nat Cell Biol*. 2021;23(2):184–197. https://doi.org/10.1038/s41556-020-00619-0
34. Martens JE, Smedts FMM, Ploeger D, et al. Distribution pattern and marker profile show two subpopulations of reserve cells in the endocervical canal. *Int J Gynecol Pathol*. 2009;28(4):381–388. https://doi.org/10.1097/PGP.0b013e31819932f8
35. Kuburich NA, den Hollander P, Pietz JT, Mani SA. Vimentin and cytokeratin: good alone, bad together. *Seminars in Cancer Biology*. 2022;86(3):816–826. https://doi.org/10.1016/j.semcancer.2021.12.006
36. Cabibi D, Eugenio Fiorentino E, Pantuso G, et al. Keratin 7 expression as an early marker of reflux-related columnar mucosa without intestinal metaplasia in the esophagus. *Med Sci Monit*. 2009;15(5):210.
37. Soares E, Zhou H. Master regulatory role of p63 in epidermal development and disease. *Cell Mol Life Sci*. 2018;75(7):1179–1190. https://doi.org/10.1007/s00018-017-2701-z
38. Pang B, Zhu Z, Xiao C, et al. Keratin 17 is required for lipid metabolism in keratinocytes and benefits epidermal permeability barrier homeostasis. *Front Cell Dev Biol*. 2022;9:779257. https://doi.org/10.3389/fcell.2021.779257
39. Nair RR, Hsu J, Jacob JT, Pineda CM, Hobbs RP, Coulombe PA. A role for keratin 17 during DNA damage response and tumor initiation. *Proc Natl Acad Sci*. 2021;118(13):e2020150118. https://doi.org/10.1073/pnas.2020150118
40. Jacob JT, Nair RR, Poll BG, et al. Keratin 17 regulates nuclear morphology and chromatin organization. *J Cell Sci*. 2020;133(20):jcs254094. https://doi.org/10.1242/jcs.254094
41. Weikel W, Wagner R, Moll R. Characterization of subcolumnar reserve cells and other epithelia of human uterine cervix: demonstration of diverse cytokeratin polypeptides in reserve cells. *Virchows Archiv B Cell Pathol Incl Mol Pathol*. 1987;54(2):98–110. https://doi.org/10.1007/BF02899201
42. Regauer S, Reich O. CK17 and p16 expression patterns distinguish (atypical) immature squamous metaplasia from high-grade cervical intraepithelial neoplasia (CIN III). *Histopathology*. 2007;50(5):629–635. https://doi.org/10.1111/j.1365-2559.2007.02652.x
43. Wang W, Lozar T, Golfinos AE, et al. Stress keratin 17 expression in head and neck cancer contributes to immune evasion and resistance to immune-checkpoint blockade. *Clin Cancer Res*. 2022;28(13):2953–2968. https://doi.org/10.1158/1078-0432.CCR-21-3039
44. Mockler D, Escobar-Hoyos LF, Akalin A, Romeiser J, Shroyer AL, Shroyer KR. Keratin 17 is a prognostic biomarker in endocervical glandular neoplasia. *Am J Clin Pathol*. 2017;148(3):264–273. https://doi.org/10.1093/ajcp/aqx077
45. Clinton LK, Miyazaki K, Ayabe A, Davis J, Tauchi-Nishi P, Shimizu D. The LAST guidelines in clinical practice: implementing recommendations for p16 use. *Am J Clin Pathol*. 2015;144(6):844–849. https://doi.org/10.1309/AJCPUXLP7XD8OQYY
46. Regauer S, Reich O, Kashofer K. Thin variant of high-grade squamous intraepithelial lesion – relationship with high-risk and possibly carcinogenic human papilloma virus subtypes and somatic cancer gene mutations. *Histopathology*. 2019;75(3):405–412. https://doi.org/10.1111/his.13869
47. Karantza V. Keratins in health and cancer: more than mere epithelial cell markers. *Oncogene*. 2011;30(2):127–138. https://doi.org/10.1038/onc.2010.456
48. Egawa N, Egawa K, Griffin H, Doorbar J. Human papillomaviruses; epithelial tropisms, and the development of neoplasia. *Viruses*. 2015;7(7):3863–3890. https://doi.org/10.3390/v7072802
49. Reich O, Regauer S. Thin HSIL of the cervix: detecting a variant of high-grade squamous intraepithelial lesions with a p16INK4a antibody. *Int J Gynecol Pathol*. 2017;36(1):71–75. https://doi.org/10.1097/PGP.0000000000000311
50. Reich O, Regauer S. Elimination of reserve cells for prevention of HPV-associated cervical cancer. *Virus Res*. 2023;329:199068. https://doi.org/10.1016/j.virusres.2023.199068
51. Burghardt E, Ostör A. Site and origin of squamous cervical cancer: a histomorphologic study. *Obstet Gynecol*. 1983;62(1):117–127.
52. Reich O, Regauer S, Gutierrez AL, Kashofer K. Copy number profiling implicates thin high-grade squamous intraepithelial lesions as a true precursor of cervical human papillomavirus-induced squamous cell cancer. *Lab Invest*. 2024;104(9):102108. https://doi.org/10.1016/j.labinv.2024.102108
53. Martens JE, Smedts F, van Muyden RCPA, et al. Reserve cells in human uterine cervical epithelium are derived from Müllerian epithelium at midgestational age. *Int J Gynecol Pathol*. 2007;26(4):463–468. https://doi.org/10.1097/pgp.0b013e31803c7c18
54. Witkiewicz AK, Hecht JL, Cviko A, McKeon FD, Ince TA, Crum CP. Microglandular hyperplasia: a model for the de novo emergence and evolution of endocervical reserve cells. *Hum Pathol*. 2005;36(2):154–161. https://doi.org/10.1016/j.humpath.2004.10.017
55. Herfs M, Soong TR, Delvenne P, Crum CP. Deciphering the multifactorial susceptibility of mucosal junction cells to HPV infection and related carcinogenesis. *Viruses*. 2017;9(4):85. https://doi.org/10.3390/v9040085
56. Marsh M, Helenius A. Virus entry: open sesame. *Cell*. 2006;124(4):729–740. https://doi.org/10.1016/j.cell.2006.02.007
57. Doorbar J, Egawa N, Griffin H, Kranjec C, Murakami I. Human papillomavirus molecular biology and disease association. *Rev Med Virol*. 2015;25(Suppl 1):2–23. https://doi.org/10.1002/rmv.1822
58. Carmichael R, Jeaffreson B. Basal cells in the epithelium of the human cervical canal. *J Pathol Bacteriol*. 1939;49(1):63–68. https://doi.org/10.1002/path.1700490108
59. Marsh M. Original site of cervical carcinoma: topographical relationship of carcinoma of the cervix to the external os and to the squamocolumnar junction. *Obstetr Gynecol*. 1956;7(4):444–452. PMID:13309917.
60. Moya J, Phillips L, Sanford J, Wooton M, Gregg A, Schuda L. A review of physiological and behavioral changes during pregnancy and lactation: potential exposure factors and data gaps. *J Expo Sci Environ Epidemiol*. 2014;24(5):449–458. https://doi.org/10.1038/jes.2013.92
61. Reich O, Pickel H, Lahousen M, Tamussino K, Winter R. Cervical intraepithelial neoplasia III: long-term outcome after cold-knife conization with clear margins. *Obstetr Gynecol*. 2001;97(3):428–430. https://doi.org/10.1016/s0029-7844(00)01174-1
62. Ferraro F, Celso CL, Scadden D. Adult stem cels and their niches. *Adv Exp Med Biol*. 2010;695:155–168. https://doi.org/10.1007/978-1-4419-7037-4_11
63. Yu WY, Slack JM, Tosh D. Conversion of columnar to stratified squamous epithelium in the developing mouse oesophagus. *Dev Biol*. 2005;284(1):157–170. https://doi.org/10.1016/j.ydbio.2005.04.042
64. Tata PR, Mou H, Pardo-Saganta A, et al. Dedifferentiation of committed epithelial cells into stem cells in vivo. *Nature*. 2013;503(7475):218–223. https://doi.org/10.1038/nature12777